

Compressive properties of Cu with different grain sizes: sub-micron to nanometer realm

Akhtar S. Khan · Babak Farrokh · Laszlo Takacs

Received: 18 September 2007 / Accepted: 29 January 2008 / Published online: 11 March 2008
© Springer Science+Business Media, LLC 2008

Abstract High-quality ultra-fine grained (ufg) and nanocrystalline (nc) bulk Cu samples of proper sizes reliable for mechanical testing, with grain sizes (d) ranging from 720 down to 22 nm were prepared by means of room temperature ball-milling and consolidation processes. The specimens were subjected to compressive loading at the quasi-static strain rate of 10^{-4} s^{-1} to large strains ($\varepsilon = 50\%$). The specimens prepared from the 10-h-milled powder ($d = 32 \text{ nm}$) were tested at a wide range of strain rates (10^{-4} to $1,860 \text{ s}^{-1}$), and the strain rate sensitivity (SRS) of the material was determined as a function of strain. The strength and work-hardening behavior were dramatically influenced by change in the grain size; the strength approached $\sim 900 \text{ MPa}$ for the 30-h-milled Cu ($d = 22 \text{ nm}$) at the strain level of $\sim 50\%$. The SRS increased several fold as the grain size was reduced to 32 nm. Further, the results obtained in this study were compared with those of other investigators on ufg and nc Cu, to gain insights into the effect of different processing routes on the investigated material properties.

Introduction

Since the landmark paper of Gleiter in 1981 [1] when he synthesized nanostructured metals using inert gas

condensation and in situ consolidation techniques, there have been hundreds of publications on different preparation and processing methods, mechanical properties, and potential applications of nanocrystalline (nc) and ultra-fine grained (ufg) materials [2]. Among ufg and nc metals and alloys, Cu has been the most widely studied material. This is evident from the efforts that have been made to report experimental results on its mechanical properties [3–18] and modeling of the constitutive behavior [19–26]. However, enormous inconsistency exists in the literature for the reported experimental data, making modeling a difficult task. For example, as reported by Weertman [27] and Cheng et al. [6], the yield strength for nc Cu ($d \approx 30 \text{ nm}$) varies over 100% (from ~ 400 to $\sim 850 \text{ MPa}$). The ambiguity is denoted more when a constitutive/ numerical model is tested for its validity/ accuracy against these spreading results [26].

It is now clear that artifacts such as porosity, impurities, and flaws introduced into the samples during the fabrication processes (especially when powders are involved, like in inert gas condensation and mechanical milling) dramatically influence the mechanical properties. In some cases, the presence of such imperfections has not even been recognized and the reported properties were attributed to the nature of ufg/nc materials [28–30].

The strength and especially the ductility of ufg/nc metals have also suffered from imperfections in test samples, both in tension and in compression. Most nc/ufg metals were not able to sustain more than a few percents of tensile plastic strain [11]. Nieman et al. [30] achieved up to 6% strain in nc Cu with 25-nm grain size, but the yield stress was very low (185 MPa). The yield stress for the tension samples of Sanders et al. [31] was higher, but the true strain was limited to 1%.

Over the last few years, different strategies have been proposed to improve the ductility (in tension) of ufg/nc

A. S. Khan · B. Farrokh (✉)
Department of Mechanical Engineering, University of Maryland
Baltimore County, 1000 Hilltop Circle, Baltimore, MD 21250,
USA
e-mail: babak2@umbc.edu

L. Takacs
Department of Physics, University of Maryland Baltimore
County, 1000 Hilltop Circle, Baltimore, MD 21250, USA

metals while maintaining the high strength [11, 32]. Recently, Youssef et al. [33, 34] reported the preparation of nc Cu using a combining liquid nitrogen and room temperature ball milling. The prepared samples had an average grain size of 23 nm and they were found to be artifact free with no residual porosity. Tension experiment on this material revealed very high yield stress (790 MPa), considerable amount of work hardening, and significant ductility, with 14% uniform elongation [34]. Cheng et al. [6] adopted the same technique with some changes in the consolidation process. They cold rolled the bulk Cu pieces to produce plate samples, centimeters in lateral directions. Their tensile experiments on the samples ($d = 54$ nm) at different quasi-static strain rates and two different temperatures exhibited elastic-perfectly plastic behavior with the yield strength of ~ 688 MPa (at room temperature and 10^{-4} s $^{-1}$), achieving a total strain of 6%.

In case of compression experiments on ufg/nc Cu, however, most of the reported results are limited to the earlier studies where either mechanical properties were dramatically influenced by the imperfections in test samples, or the specimens were so small in size that the existence of uniaxial stress state during the tests could not be assured. Further, in most cases, the reported data was restricted to experiments at only one strain rate at room temperature and only for a single grain size.

Suryanarayanan et al. [13] performed uniaxial compression experiments at a strain rate of 10^{-3} s $^{-1}$ on nc samples obtained via solution-phase synthesis and consolidation. The samples were $2.5 \times 2 \times 3.5$ mm in size, their density was 90–92% of the theoretical value, and the grain size was between 39 and 54 nm. They reported ~ 400 MPa yield strength and total strains of $\sim 25\%$. Improved sample preparation produced more dense samples (98% of the theoretical density) with smaller average grain size (27 nm) [14]. Disk samples with 13-mm diameter and 5–10-mm thickness exhibited slightly higher yield and flow stress [14, 15]. Champion et al. [8] produced nc Cu ($d = 50$ nm) by cryo-melting, cold isostatic pressing (CIP), sintering and extrusion. The sample (cylindrical specimen of 4-mm diameter and 5-mm length, with 90% of the theoretical density) was subjected to compression experiments at 10^{-4} s $^{-1}$ ($\sigma_y = 470$ MPa). They reported maximum strain measurements of 18%; whereas, elucidated that due to the unreliability of strain measurements the obtained results were semi-quantitative. Haouaoui et al. [18] prepared Cu samples of different grain sizes by consolidating micro- and nano-powders using equal channel angular extrusion (ECAE). Although the samples exhibited relatively high strength (σ_y up to 560 MPa), the ductility was rather low ($\varepsilon < 10\%$). Other results on compressive properties of ufg and nc Cu can be found elsewhere [9, 10, 12, 16].

In this study, an effort has been made to prepare high quality samples in a wide range of grain sizes (from sub-micron to nanometer range), with a size suitable for uniaxial compression testing. This was accomplished by modifying the technique employed by Khan et al. earlier [17, 35, 36]. The effect of the grain size on the mechanical properties, such as micro-hardness, compressive yield stress, flow stress, and strain rate (quasi-static to dynamic) sensitivity, are investigated and compared with data available in the literature.

Experimental procedure

Preparing ultra-fine grained and nanocrystalline samples

Cu powder (-325 mesh, 99.63% pure) was obtained from Alfa Aesar[®]. The powder was first degassed (dried) for 7 h under vacuum at 520 K. Subsequent handling of the powder was carried out in a stainless steel glove box filled with argon; the residual oxygen level was below 3 ppm. The powder and hardened steel balls (12.5 mm in diameter) were placed in 0.5 L steel containers and sealed inside the glove box. About 47.5 g of Cu powder and 95 steel balls (~ 760 g) were used, corresponding to a ball-to-powder ratio (BPR) of 16:1. Small amounts of stearic acid ($\text{CH}_3(\text{CH}_2)_{16}\text{COOH}$) were added to serve as the process control agent (PCA) to prevent excessive cold welding. Ball milling was carried out using a Fritsch Pulverisette-5 planetary mill. The speed of the mill was set to 120 rpm. To obtain samples with different grain sizes, the milling time was varied from 0.5 to 30 h. Table 1 lists the milling times and the corresponding amount of PCA used for each sample. The milling was carried out at room temperature; however, to avoid a significant temperature rise, 15 min of milling was alternated with 15 min of cooling through the built-in fans of the system.

To achieve the material in bulk form, the prepared powder was loaded into a hollow cylindrical die inside the glove box; the die consisted of a cylinder made of heat-treated Vasco-Max C-350 with inner and outer diameters of 22 and 54 mm, respectively, a cylindrical split die which allowed the easy removal of the specimen from the die after consolidation processes, and plungers to consolidate the powder from top and bottom symmetrically. The inner surfaces of the cylindrical split inserts were lubricated with

Table 1 The milling times of Cu powder and the amount of PCA used for each period

Milling time (h)	0.5	2	5	10	20	30
Stearic acid (% wt.)	0.01	0.1	0.12	0.2	0.3	0.5

Teflon[®] spray to reduce the effect of friction forces during consolidation. The powder was pre-cold-compacted inside the glove box using a 4-ton bottle jack. The initial green body resulting from the pre-compaction process was isolated by thin layers of graphite powder on both ends to prevent the penetration of oxygen and other impurities during the subsequent consolidation processes. The sealed die including the green body was removed from the glove box and subjected to higher compacting pressure of 2.1 GPa at room temperature for 10 min. To achieve higher density, eliminate adsorbates and enhance proper interparticle bonding [37], the material was warm compacted at 703 K for 1 h while still subjected to axial stress of 1.2 GPa. It is worthwhile mentioning that the parameters of the consolidation process (applied stress and temperature) were kept the same for the preparation of each sample. Using this technique, specimens from as-received (degassed) powder, 0.5-, 2-, 5-, 10-, 20- and 30-h-milled powders were prepared for quasi-static compression experiments. The samples after removal from the die (Fig. 1a) were machined to cylindrical specimens in unique sizes of 8.9 and 9.9 mm in diameter (D) and length (L) with $L/D > 1$, respectively (Fig. 1b). In contrast to many studies in the field in which the small size of specimens did not allow the use of an accurate strain measurement technique [8, 9, 28, 38] the reasonable size of samples in this work permitted the use of high elongation

strain gages (KFEL-2-120-C1, Kyowa Ltd.), resulted in precise measurement of strains. In addition, a disk sample, 8.9 mm in diameter and ~ 3 -mm thick, was prepared for the uniaxial high strain rate experiment, using the split Hopkinson pressure bar (SHPB) technique.

Grain size measurement and powder contamination

The average grain size of the milled powders and the consolidated samples were evaluated through the X-ray diffraction analysis using a Philips X'Pert diffractometer operating in the θ - θ geometry with $\text{CuK}\alpha$ ($\lambda = 0.154$ nm) radiation. The linewidths were determined after numerically removing the contribution of the $\text{K}\alpha_2$ radiation and correcting for instrumental broadening. The average grain size and the lattice strain were separated using the different diffraction angle dependence of the corresponding contributions to the integral linewidth.

Iron contamination has always been a concern in mechanical milling [6, 39, 40]. Undesirable wearing and tearing of the steel-grinding medium and the vial during the milling process result in the incorporation of iron particles (iron contamination) into the powder [39]. El-Eskandarany et al. [40] detected up to 5% iron contamination in their mechanically alloyed Al–50 at% Ta powder. More recently, Cheng et al. [6], observed $\sim 2.3\%$ iron contamination in their 25-h-milled Cu powder. To investigate the iron contamination and other impurities in the prepared samples energy-dispersive X-ray analysis (EDXA) was performed using a JSM-5600 SEM system, equipped with a high resolution silicon X-ray detector. The system resolution was 129 eV. The measurements were performed identically on bulk specimens prepared from the as-received powder and those consolidated from 5-, 10- and 30-h of milled powder products. The spot size (probe size) was set to be 60 with a magnification of $500\times$ and the accelerating voltage of 20 keV. The analysis was performed in the following steps: specimens were first quantified to detect all the existing elements using the 'Auto ID' feature of the system; samples were manually tested for different elements, such as, Al, Ar, Sc, Ti, V, Cr, Mn, Fe, Co, Ni, Zn, etc. and finally the materials were analyzed to detect only Cu and Fe (the most probable contaminating element).

Mechanical property characterization

To examine the uniformity of the bulk samples and to evaluate the capability of the employed consolidation technique, the micro-hardness of a 10-h-milled bulk sample at 15 different equally spaced spots (0.56 mm apart) across the diameter, on four different circular surfaces along the length of specimen was measured using the Buehler I micro-hardness tester (inserts of Fig. 3).

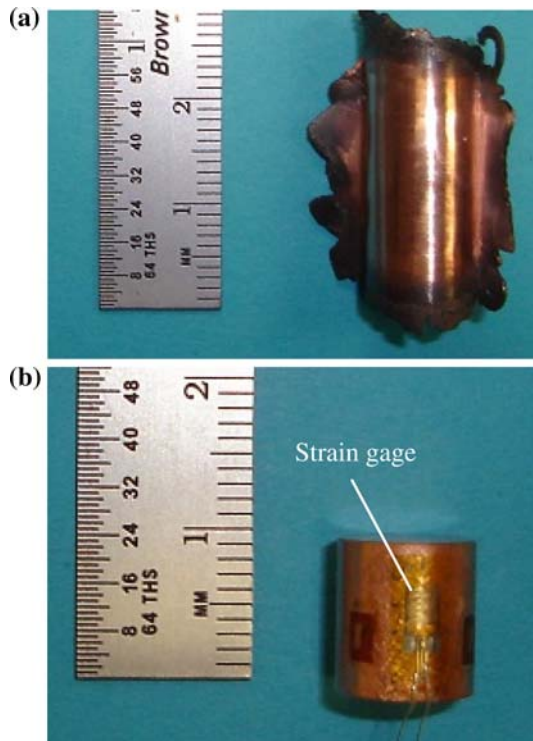


Fig. 1 The consolidated ball-milled Cu sample (a) after removal from the die and (b) after machining and high elongation strain gage installation

To investigate the effect of grain refinement on mechanical properties of bulk Cu, quasi-static uniaxial compression experiments at a strain rate of 10^{-4} s^{-1} were performed on specimens prepared from as-received, 0.5-, 2-, 5-, 10-, 20- and 30-h-milled powders. Also, to determine the strain rate sensitivity (SRS) of the nc bulk Cu, quasi-static compression experiments at strain rates of 10^{-4} , 10^{-2} , and 1 s^{-1} and a high strain rate (dynamic) experiment were performed on samples prepared after 10 h of milling. An MTS 809 Axial/Torsional Material Testing System and the split Hopkinson pressure bar (SHPB) technique were used for performing all quasi-static and dynamic experiments, respectively. The details of similar experiments with other materials can be found elsewhere [41–43].

Results and discussion

Material characterization (grain size, lattice strain, contamination, and homogeneity)

The average grain sizes determined from the linewidths of the X-ray diffraction patterns are presented in Table 2 for both the as-milled powders and the consolidated samples. An average grain growth of about 30% was observed as the result of the consolidation processes. This however was unavoidable; as the application of high pressure and temperature during the consolidation process was necessary to achieve high density, eliminate adsorbates, and enhance proper interparticle bonding [37]. The densities of the bulk samples were measured to be between 96% and 98% of the Cu theoretical value. The average lattice strain for all prepared samples was evaluated to be less than 0.1%, indicating that the samples were substantially annealed during the warm compaction of 60 min at 703 K.

Figure 2 illustrates the results from the energy-dispersive X-ray analysis (EDXA) of the samples prepared from the as-received (–325 mesh), 5-, 10- and 30-h-milled Cu powders. Comparing Fig. 2a, the EDXA result of as-received consolidated sample, with those prepared after several hours of milling (Fig. 2b–d) shows no significant differences, implying that the milling process did not introduce additional impurities to the specimens. Although, the EDXA detected Cu as the only element present in the consolidated samples (even after 30 h of milling) in all

steps, it is possible that the prepared samples had some small amounts of impurities that could affect the mechanical properties of the material. Possible impurities contributed by the milling tools (Fe), atmosphere (O and Ar), the utilized PCA, and those from starting powder ($\sim 0.37\%$ impurity; the starting powder was 99.63% pure) were below the detection limit of $\sim 1\%$ and atomic number 12 of the EDXA technique. It is anticipated that the proper use of the PCA along with the Cu powder has efficiently prevented the iron contamination from the milling tools. Similar effect has been reported by Mishura et al. [44] and also by Gaffet et al. [45], where application of different PCAs decreased the iron contamination during the milling process.

Figure 3 shows the Vicker's hardness values along the diameter of a 10-h-milled ($d = 32 \text{ nm}$) bulk sample measured on four different circular surfaces through the length of the cylindrical specimen. The data population with the standard deviation ranging from 0.07 to 0.14 GPa indicates the fact that the material had almost identical properties all through the specimen, confirming the homogeneity of the prepared sample and the applicability of the consolidation technique.

Mechanical properties

Grain size dependence of yield and flow stress

Figure 4 shows the stress–strain response of the ball-milled bulk Cu for different average grain sizes ranging from 720 down to 22 nm at the strain rate of 10^{-4} s^{-1} . For comparison, response of the coarse-grained (CG) annealed oxygen-free high conductivity (OFHC) Cu [46] is included. It is clear that the strength and work-hardening behavior are dramatically influenced by refining the grains. The yield stress reached $\sim 680 \text{ MPa}$ for the smallest grain size of 22 nm. This is however $\sim 14\%$ lower than the value reported by Youseff et al. [34] for the ball-milled nc Cu ($d = 23 \text{ nm}$) under tension. The lower yield stress in the material is attributed to the annealed-state and hence the lower dislocation density in the material as compared with severely deformed Cu of Youssef et al. It is evident (Fig. 4) that the materials showed some strain-hardening behavior even for the samples with the smallest grains. More significant work-hardening behavior, however, was observed by Youssef et al. [34] for nc Cu in tension. More recently,

Table 2 The results of X-ray diffraction analysis (average grain size measurement) for mechanically milled Cu powders and bulk samples

Milling Type	Milling time (h)						
	0	0.5	2	5	10	20	30
Powder	8–11 μm APS ^a	252 nm	84 nm	35 nm	25 nm	19 nm	14 nm
Bulk specimen (nm)	720	350	118	51	32	27	22

^a APS: average particle size

Fig. 2 The results from energy-dispersive X-ray analysis (EDXA) for the ball milled bulk Cu samples; for (a) as received (un-milled) material, and after (b) 5 h, (c) 10 h, and (d) 30 h of milling

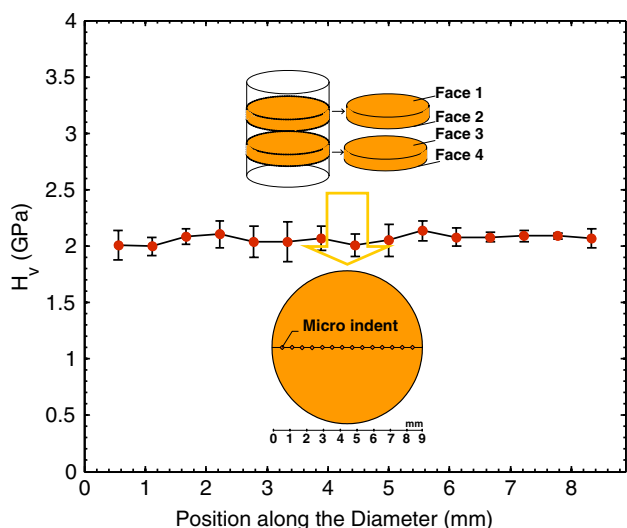
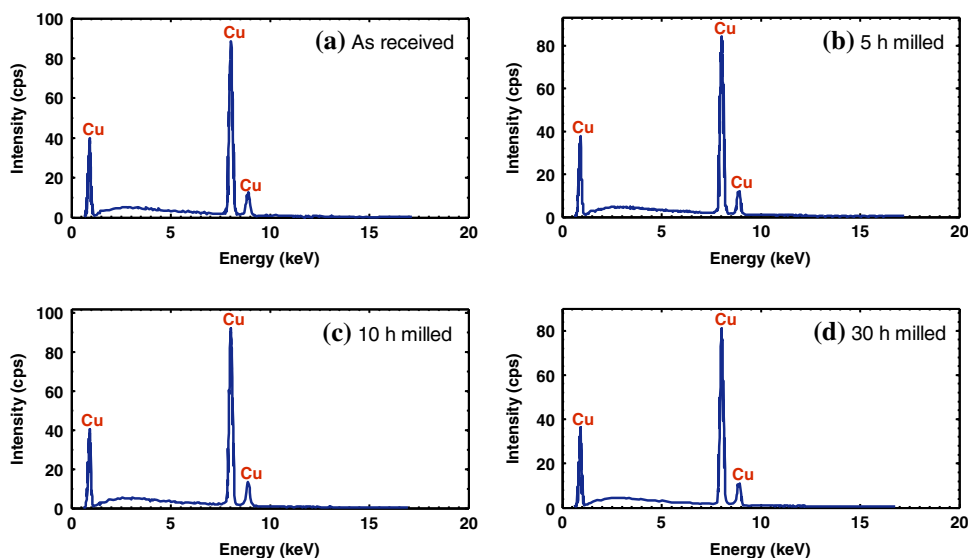


Fig. 3 Vicker's hardness measurements throughout the 10 h-milled ($d = 32$ nm) bulk Cu specimen

Guduru et al. [47] reported that the in situ deformation studies conducted in a TEM on this material revealed dislocation pile ups even in smaller grains, and the presence of dislocation activity was assumed to be responsible for the observed strain hardening. This work-hardening response, however, is different from those which have been observed for many nc and ufg metals; in these materials, the stress-strain curves (in tension and compression) show a rapid strain hardening in the early stages of plastic deformation followed by a wide flat region with little or no strain-hardening behavior in the later stages [6, 47]. It is believed that the faster strain-hardening rate in the early stages of plastic deformation is due to the dislocation activity in larger grains. The larger grains in the material saturate after a certain extent of plastic deformation, while in smaller

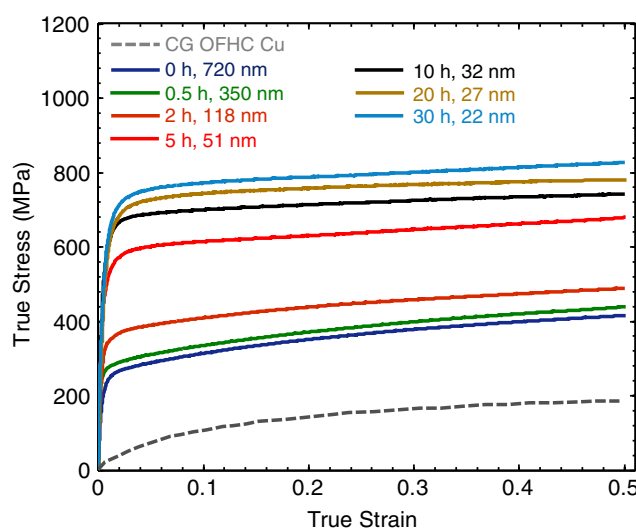


Fig. 4 The effect of grain size (milling time) on the compressive uniaxial stress-strain response of mechanically milled bulk Cu at the strain rate of 10^{-4} s^{-1}

grains the dislocation activity is very limited. Therefore, the total decrease in dislocation activity in early stages of plastic deformation prevents the strain hardening from taking place, which results in an elastic-perfectly plastic behavior of these materials [6, 10, 47–49]. Thus, as stated by Guduru et al. [47], the strain-hardening behavior observed in the ball-milled bulk Cu in this study and that of Youssef et al. [34] is contrary to the foregoing theory; the possible reasons of such differences are not clear at this time.

The response of the 30-h-milled ($d = 22$ nm) Cu of this study (curve O) is compared in Fig. 5 with other uniaxial compressive stress-strain data available on Cu with grain sizes smaller than 300 nm (curve A shows data on CG OFHC Cu for comparison). Note that in this figure, the dashed lines represent the responses of those materials consolidated from

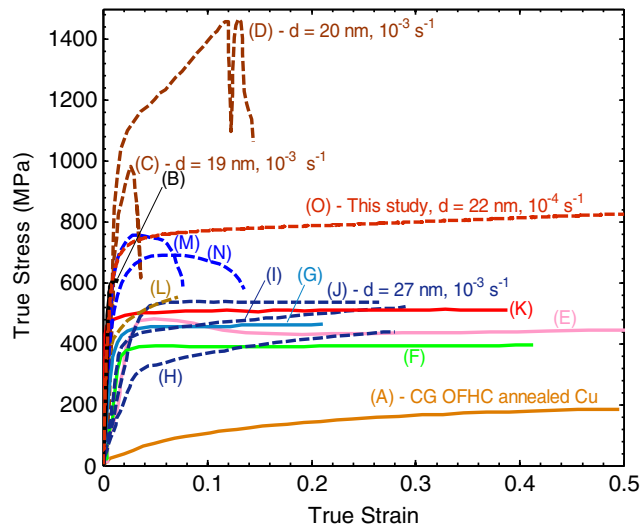


Fig. 5 Uniaxial compression experimental results of CG, ufg and nc Cu at quasi-static strain rates reported in literature in comparison with the response of nc Cu of this study. Note that the dashed-lines indicate results from experiments in which samples were prepared through powder (or particles) consolidation; whereas, solid-lines represent the responses of those samples prepared from other synthesizing techniques as described below: A—Tanner et al., CG OFHC annealed Cu at 0.0004 s^{-1} [46]; B—Champion et al., nc Cu prepared through cryomelting, compaction and extrusion, with average $d = 50 \text{ nm}$ at 0.0001 s^{-1} [8]; C and D—Youngdahl et al., nc Cu prepared through inert gas condensation and compaction with $d = 19\text{--}20 \text{ nm}$ at 0.001 s^{-1} [9]; E—Wang and Ma, ufg Cu processed through cryorolling with $d = 200\text{--}300 \text{ nm}$ at 0.0001 s^{-1} [10]; F—Wang and Ma, ufg Cu by ECAP with $d = 300 \text{ nm}$ at 0.001 s^{-1} [11]; G—Gray et al., ufg Cu by ECAP with $d = 300 \text{ nm}$ at 0.001 s^{-1} [12]; H, I, and J—Suryanarayanan et al., nc Cu synthesized through solution-phase synthesis and compaction with $d = 54, 39$ and 27 nm at 0.001 s^{-1} , respectively [13–15]; K—Valiev et al., ufg Cu by ECAP, $d = 210 \text{ nm}$ at 0.0014 s^{-1} [16]; L—Khan et al., nc Cu by ball milling (60 h) and compaction, at 0.0001 s^{-1} [17]; M and N—Haouaoui et al., ufg Cu by ECAE of powder with $d = 140$ and 110 nm at 0.0005 s^{-1} , respectively [18]; O—This study, $d = 22 \text{ nm}$ at 0.0001 s^{-1}

a powder or small particles. Compared with samples in the same grain size range, our 30-h-milled Cu exhibited high strength, yet sustaining considerable ductility. The curves C and D of Youngdahl et al. [9] exhibited higher strength and extreme work-hardening behavior, yet much lower ductility as compared with the curve O of this study (Fig. 5). These compressive stress–strain data (curves C and D) are somewhat questionable; Wang and Ma [10] reported that the observed work-hardening behavior was due to the inadvertent misuse of the tensile formula when converting the engineering stress to true stress.

Figure 6 shows the 0.2% off-set compressive yield stress for Cu as a function of grain size showing our results compared to data available in literature. The solid line represents the extrapolation of the Hall–Petch equation for CG Cu [51]. As it is clearly evident from this plot, the yield stresses followed the solid line, indicating the validity of the Hall–Petch relation for this range of grain sizes.

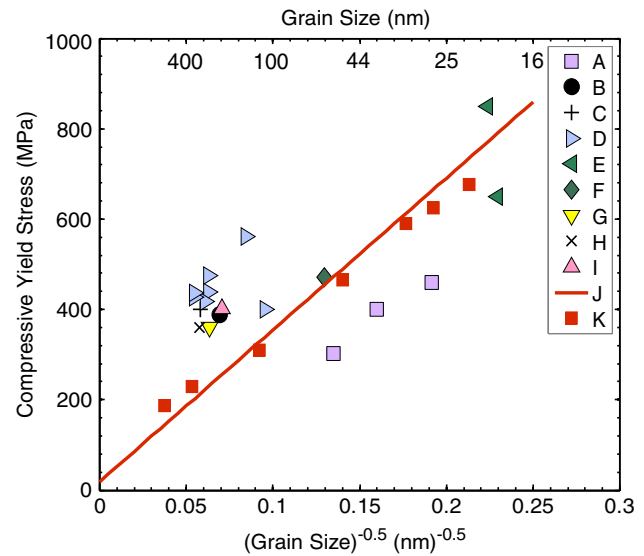


Fig. 6 Summary of compressive yield stress experimental data reported in literature for fine-grained to nc Cu in comparison with those measured from the ball-milled bulk Cu samples of this study. Note that all data were evaluated from the uniaxial compressive experiments performed at quasi-static strain rates. A—Suryanarayanan et al. [13–15]; B—Valiev et al. [16]; C—Gray et al. [12]; D—Haouaoui et al. [18]; E—Youngdahl et al. [9]; F—Champion et al. [8]; G—Wang and Ma [10]; H—Wang and Ma [11]; I—Smirnov et al. [50]; J—The extrapolation of the Hall–Petch relation evaluated for larger grains, Meyers and Chawla [51]; K—This study

Strain rate sensitivity (SRS)

Figure 7 illustrates the uniaxial compressive stress–strain response of the 10-h-milled bulk nc Cu ($d = 32 \text{ nm}$) at different quasi-static strain rates of 10^{-4} , 10^{-2} , and 1 s^{-1} , and a dynamic strain rate of $1,860 \text{ s}^{-1}$. The results indicated a pronounced positive strain rate sensitivity of the

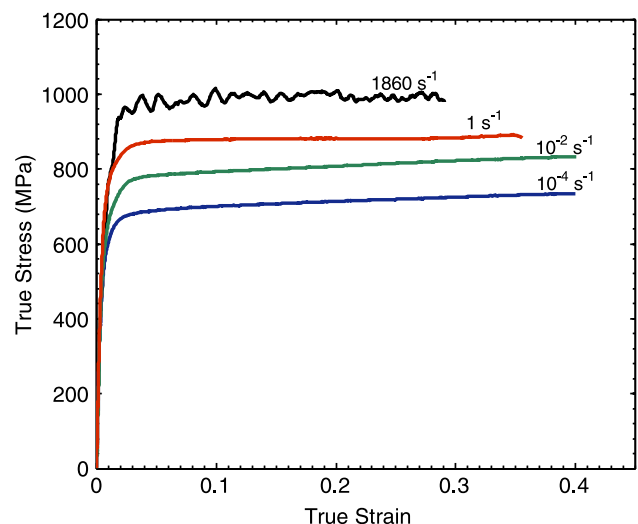


Fig. 7 The compressive stress–strain response of 10 h-milled ($d = 32 \text{ nm}$) nc Cu at quasi-static and dynamic strain rates

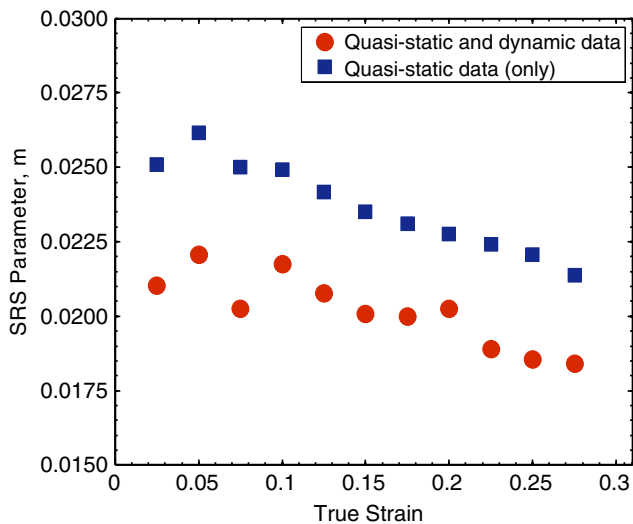


Fig. 8 The strain rate sensitivity (SRS) of 10-h-milled Cu ($d = 32$ nm) as a function of strain

material. In practice, several experimental techniques have been used to evaluate the SRS of the parameter quantitatively. However, evaluating the SRS parameter m by means of strain rate jump test, a series of uniaxial monotonic experiments at different strain rates, or stress relaxation experiment are among the widely used methods [52]. In the current study, results in Fig. 7 were used to calculate the SRS parameter for the 10-h-milled ($d = 32$ nm) Cu. The m value, a quantity to assess the thermodynamic and kinetics aspects of plastic deformation of the material [52], defined as:

$$m = \frac{\partial \ln \sigma_f}{\partial \ln \dot{\epsilon}} \quad (1)$$

where σ_f and $\dot{\epsilon}$ are the flow stress and strain rate, respectively, was evaluated as a function of true strain and is shown in Fig. 8. The dependency of SRS on strain is evident from the data; an almost linear decrease in SRS with deformation is notable. This dependency, however, was not considered while evaluating the strain rate sensitivity of many nc materials. In most studies, the strain rate jump experiments at a constant temperature were conducted to evaluate the SRS parameter; applying this method, m value could be evaluated by employing only one sample test. In this case, the SRS parameter is obtained by using the following equation [52]:

$$m = \frac{\Delta \ln \sigma_f}{\Delta \ln \dot{\epsilon}} \quad (2)$$

In this technique, the m value is inevitably an average along the strain range, or could be evaluated for only two subsequent strain rates (before and after the strain rate jump). However, applying Eq. 1 to the results from the uniaxial experiments (at different strain rates) of this study

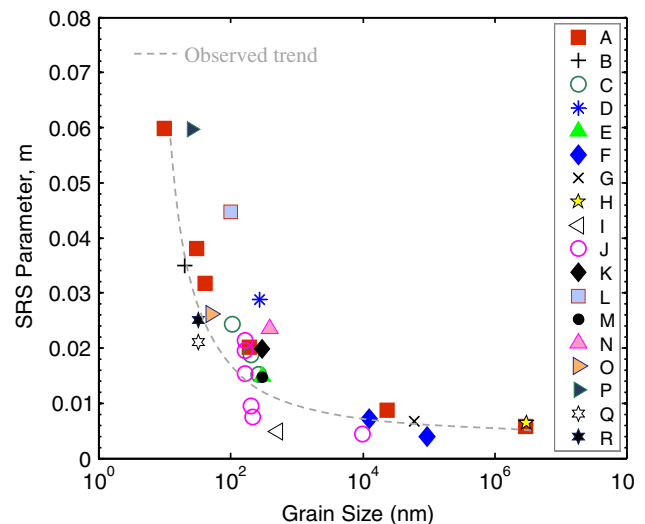


Fig. 9 The Cu strain rate sensitivity (SRS) parameter values as a function of grain size evaluated through different experimental techniques as compared with those evaluated in this study from wide range of strain rates (including a dynamic test) at the strain level of 0.025. A—Chen et al. [3]; B—Lu et al. [53]; C—Wei et al. [54]; D—Elmustafa et al. [55]; E—Gray et al. [12]; F—Carreker and Hibbard [56]; G—Zehetbauer and Seumer [57]; H—Bochniak [58]; I—Lu et al. [59]; J—Torre et al. [60]; K—Elmustafa et al. [61]; L—Valiev et al. [62]; M—Wang and Ma [5]; N—Li and Blum [63]; O—Cheng et al. [6]; P—Jiang et al. [64]; Q—This study, from both quasi-static and dynamic strain rates; R—This study, from quasi-static strain rates only

resulted in calculating the m value as a function of strain to a relatively large value ($\sim 28\%$). Further, in most investigations the influence of high strain rate response of the material on the SRS behavior was not considered; the reported values were mainly limited to quasi-static strain rates. Figure 8 illustrates the fact that the ignorance of the latter could cause an average variation of 17% to the evaluated m values. Figure 9 summarizes the SRS of Cu of different grain sizes evaluated from various experimental techniques. For comparison the m values of this study calculated at 2.5% strain (data point Q—from quasi-static and dynamic strain rates, and data point R—from quasi-static strain rates only) were also plotted against the existing literature data. The evaluated SRS of the material followed the same trend as shown in this figure. However, slightly lower SRS of the material in this study as compared with Cu with grains in the same size range could be attributed to lower dislocation density of the material; as mentioned earlier, application of relatively high temperature/pressure during the consolidation processes caused annealing and some grain coarsening in the material. This however has been predicted by Wei et al. model [54] for the thermally activated dislocation processes in FCC metals by considering the length scales in nc grains during grain boundary-dislocation interactions. The model in general states that the m increases with increasing cold work and refined grain structures. This supports the experimentally observed

increase in SRS as the result of grain refinement for other FCC metals (e.g., Ni and Al) as well [52, 54, 65–68].

Micro-hardness

Figure 10 summarizes the Vicker's hardness values of the Cu of this work (data points M) of different grain sizes along with hardness values reported in the literature. The solid line represents the approximated hardness ($H \approx 3\sigma_y$ —Tabor relation [75]) from the extrapolated Hall–Petch relation for CG Cu [51]. Although the hardness values of this study could be fitted to an almost straight line (dashed line), however, they deviated from the Hall–Petch equation for hardness. This deviation, however, became negligible as the material grain sizes decreased into nanometer realm. The possible reason for this observation could be attributed to the fact that the Tabor relation, that is the indentation hardness is three times the yield stress, is valid only for those materials exhibiting perfectly plastic (or extremely low work hardening) behavior [76]. For bigger grains the material exhibits a more pronounced work-hardening behavior (see Fig. 4) and the Tabor relation is not reliable for predicting the yield behavior of materials. Note that some data (e.g., data points D and J) show much higher hardness than the values predicted by the Hall–Petch relation. The possible reason as stated by Dao et al. [77] is due to the fact that these samples were prepared via severe plastic deformation, in which dense dislocation walls, tangles, cell walls or sub-grain

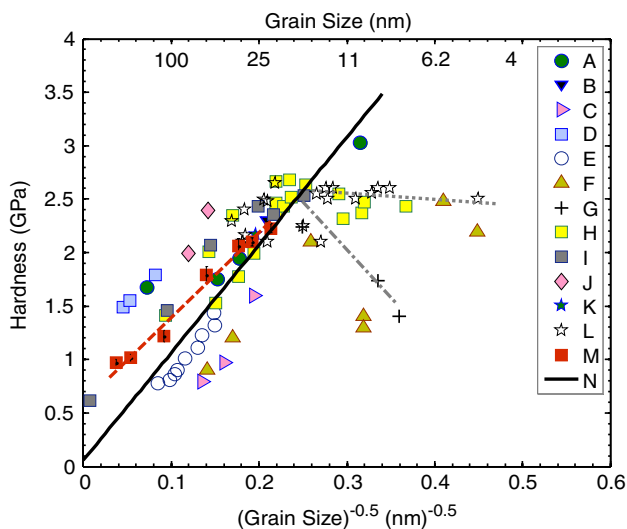


Fig. 10 The hardness values reported in literature for ufg and nc Cu in comparison with those measured in this study. A—Chen et al. [3]; B—Youssef et al. [33]; C—Suryanarayanan et al. [13]; D—Jiang et al. [69]; E—Das et al. [70]; F—Nieman et al. [30]; G—Chokshi et al. [71]; H—Sanders et al. [31]; I—Youngdahl et al. [9]; J—Ganapathi et al. [72]; K—Shen et al. [73]; L—Fougere et al. [74]; M—This study; N—Hall–Petch equivalent [51, 75] (Tabor relation)

boundaries were formed; these were barriers to the motion of dislocations and strengthened the materials. At the grain sizes of about 16 nm and smaller, the change in hardening trend is clearly visible (except for data point A). In this region the softening in the material (with decrease in the average grain size) with different trends (dotted-line and chain-line in Fig. 10) has been noticed. The interpretation of the observed experimental results, however, is a matter of controversy in the field; some investigators attributed this to change in the deformation mechanism below a critical grain size (the inverse Hall–Petch effect) [78], while the others kept the effect of processing routes (i.e., porosities, improper bonding, impurities, etc.) responsible for the softening behavior [4].

Conclusions

Sub-micron grained and nanocrystalline high-quality bulk Cu specimens were prepared through mechanical milling and consolidation processes. Based on the results from this experimental study, the following conclusions were drawn:

1. The proper use of PCA along with the Cu powder during the milling process substantially reduced the iron contamination of the milled powder and subsequently the bulk specimens.
2. The average grain growth of $\sim 30\%$ was observed as the result of relatively high temperature and pressure during the consolidation process. On the other hand, highly dense and adsorbate-free specimens were obtained that exhibited high strength and ductility.
3. The relatively large size of specimens allowed the use of high elongation strain gages that provided accurate strain measurements (in elastic and plastic regimes) during the experiments.
4. The strength was dramatically influenced by grain refinements and followed the Hall–Petch prediction down to the grain size of 22 nm.
5. The work hardening and its rate also reduced as the material grain size was decreased to nano-meter realm.
6. The effect of not considering the dynamic strain rate response while evaluating the strain rate sensitivity of the material resulted in $\sim 17\%$ variation in the reported m value.
7. The slightly lower strain rate sensitivity of the 32-nm Cu as compared with those in the same size range grains was attributed to lower dislocation density of the material which was predicted by Wei et al. theory [54].

Acknowledgement The co-author, Babak Farrokh, gratefully acknowledges the support from the U.S. Department of Education through the Graduate Assistance in Areas of National Need (GA-ANN) Fellowship.

References

1. Gleiter H (1981) Materials with ultrafine grain size. In: Hansen N (ed) Deformation of polycrystals: mechanisms and microstructures. Risø National Laboratory, Roskilde, p 15
2. Meyers MA, Mishra A, Benson DJ (2006) Prog Mater Sci 51:427
3. Chen J, Lu L, Lu K (2006) Scripta Mater 44:1913
4. Meyers MA, Mishra A, Benson DJ (2006) JOM 58:41
5. Wang YM, Ma E (2003) Appl Phys Lett 83:3165
6. Cheng S, Ma E, Wang YM, Kecskes LJ, Youssef KM, Koch CC, Trociewitz UP, Han K (2005) Acta Mater 53:1521
7. Wei X, Lee D, Shim S, Chen X, Kysar JW (2007) Scripta Mater 57:541
8. Champion Y, Guérin-Mailly S, Bonnentien JL, Langlois P (2001) Scripta Mater 44:1609
9. Youngdahl CJ, Sanders PG, Eastman JA, Weertman JR (1997) Scripta Mater 37:809
10. Wang YM, Ma E (2004) Mater Sci Eng A 375–377:46
11. Wang YM, Ma E (2004) Acta Mater 52:1699
12. Gray GT III, Lowe TC, Cady CM, Valiev RZ, Aleksandrov IV (1997) Nanostruc Mater 9:477
13. Suryanarayanan Iyer R, Frey CA, Sastry SML, Waller BE, Bhuro WE (1999) Mater Sci Eng A 264:210
14. Suryanarayanan R, Frey CA, Sastry SML, Waller BE, Bates SE, Buhro WE (1996) J Mater Res 11:439
15. Suryanarayanan R, Frey CA, Sastry SML, Waller BE, Buhro WE (1996) Deformation behavior of nanocrystalline Cu and Cu–0.2 wt%B produced by hot pressing of solution phase synthesis. In: Suryanarayana C, Singh J, Froes H (eds) Processing and properties of nanocrystalline materials, p 407
16. Valiev RZ, Kozlov EV, Ivanov YF, Lian J, Nazarov AA, Baudelet B (1994) Acta Metall Mater 42:2467
17. Khan AS, Zhang H, Takacs L (2000) Int J Plast 16:1459
18. Haouaoui M, Karman I, Maier HJ, Hartwig KT (2004) Metall Mater Trans A 35:2935
19. Mercier S, Molinari A, Estrin Y (2007) J Mater Sci 42:1455
20. Conrad H (2003) Mater Sci Eng A 341:216
21. Wei Y, Su C, Anand L (2006) Acta Mater 54:3177
22. Schiøtz J (2004) Scripta Mater 51:837
23. Lian J, Baudelet B, Nazarov AA (1993) Mater Sci Eng A 172:23
24. Pande CS, Masumura RA, Marsh SP (1997) Acta Mater 45:4361
25. Jiang B, Weng GJ (2004) J Mech Phys Solids 52:1125
26. Fu HH, Benson DJ, Meyers MA (2004) Acta Mater 52:4413
27. Weertman JR (2002) In: Koch CC (ed) Nanostructured materials: processing, properties and applications. William Andrews Publishing, Norwich (NY), p 397
28. Sanders PG, Youngdahl CJ, Weertman JR (1997) Mater Sci Eng A 234:77
29. Krstic V, Erb U, Palumbo (1993) Scripta Mater 29:1501
30. Nieman GW, Weertman JR, Siegel RW (1991) J Mater Res 6:1012
31. Sanders PG, Eastman JA, Weertman JR (1997) Acta Mater 10:4019
32. Koch CC (2003) Scripta Mater 49:657
33. Youssef KM, Scattergood RO, Murty KL, Koch CC (2004) Appl Phys Lett 85:929
34. Youssef KM, Scattergood RO, Murty KL, Horton JA, Koch CC (2005) Appl Phys Lett 87:091904-1
35. Khan AS, Zhang H (2000) Int J Plast 16:1477
36. Khan AS, Suh YS, Chen X, Takacs L, Zhang H (2006) Int J Plast 22:195
37. Groza JR (2002) In: Koch CC (eds) Nanostructured materials: processing, properties, and applications. Noyes Publication, Norwich (NY), p 115, (Chap 4)
38. Ko SH, Jang JM, Lee W (2005) Mater Sci Forum 475–479:3489
39. Suryanarayana C (2004) Mechanical alloying and milling. Marcel Dekker, New York (NY), p 385, (Chap 15)
40. El-Eskandarany S, Aoki M, Itoh K, Suzuki K (1991) J Less Common Metals 169:235
41. Khan AS, Farrokh B (2006) Int J Plast 22:1506
42. Khan AS, Kazmi R, Farrokh B, Zupan M (2007) Int J Plast 23:1105
43. Khan AS, Liang R (1999) Int J Plast 15:1089
44. Mishra JC, Suryanarayana C, Froes HF, ID (1994) University of Idaho. In: Mechanical alloying and milling. C. Suryanarayana (2004), author. Marcel Dekker, p 400
45. Gaffet E, Harmelin M, Faudot F (1993) J Alloys Compd 194:23
46. Tanner AB, McGinty RD, McDowell DL (1999) Int J Plast 15:575
47. Guduru RK, Murty KL, Youssef KM, Scattergood RO, Koch CC (2007) Mater Sci Eng A 463:14
48. Wang Y, Chen M, Zhou F, Ma E (2002) Nature 419:912
49. Ma E (2003) Scripta Mater 49:663
50. Smirnov BI, Shpeizman VV, Nikolaev VI (2005) Phys Solid State 47:840
51. Meyers MA, Chawla KK (1999) Mechanical behavior of materials. Prentice-Hall, Upper Saddle River (NJ), p 271
52. Wei Q (2007) J Mater Sci 42:1709
53. Lu L, Li SX, Lu K (2001) Scripta Mater 45:1163
54. Wei Q, Cheng S, Ramesh KT, Ma E (2004) Mater Sci Eng A 381:71
55. Elmustafa AA, Tambwe MF, Stone DS (2003) MRS Symp Proc 70:Y8.14.1
56. Carreker RP Jr, Hibbard WR Jr (1953) Acta Metall 1:654
57. Zehetbauer M, Seumer V (1993) Acta Metall 41:577
58. Bochniak W (1995) Acta Metall 43:225
59. Lu L, Schwaiger R, Shan ZW, Dao M, Lu K, Suresh S (2005) Acta Mater 53:2169
60. Torre FD, Pereloma EV, Davies CHJ (2006) Acta Mater 54:1135
61. Elmustafa AA, Tambwe MF, Stone DS. Activation volume analysis of plastic deformation in fcc materials using nanoindentation. Presented at surface engineering 2002-synthesis, characterization and applications, MRS Fall Meeting, Boston, MA
62. Valiev RZ, Alexandrov IV, Zhu YT, Lowe TC (2002) J Mater Res 17:5
63. Li YJ, Blum W (2005) Phys Status Solidi A 202:R119
64. Jiang Z, Liu X, Li G, Jiang Q, Lian J (2006) Appl Phys Lett 88:14115-1
65. Miyamoto H, Ota K, Mimaki T (2006) Scripta Mater 54:1721
66. Hoppel HW, May J, Eisenlohr P, Goken M (2005) Zeit fur Metallkunde 96:566
67. Pan D, Nieh TG, Chen MW (2006) Appl Phys Lett 88:1119
68. Wang YM, Hamza AV, Ma E (2006) Acta Mater 54:2715
69. Jiang HG, Zhu YT, Butt DP, Alexandrov IV, Lowe TC (2000) Mater Sci Eng A 290:128
70. Das D, Samanta A, Chattopadhyay (2006) Synth React Inorg, Metal-Organ Nano-Metal Chem 36:221
71. Chokshi H, Rosen A, Karch J, Gleiter H (1989) Scripta Metall 23:1679
72. Ganapathi SK, Aindow M, Fraser HL, Rigney DA (1991) MRS Symp Proc 206:593
73. Shen TD, Koch CC, Tsui TY, Pharr GM (1995) J Mater Res 10:2892
74. Fougere GR, Weertman JR, Siegel RW, Kim S (1992) Scr Metall 26:1879
75. Tabor D (1951) J Inst Metals 79:1
76. Gerck AP (1997) J Mater Sci 12:735
77. Dao M, Lu L, Asaro RJ, De Hosson JTM, Ma E (2007) Acta Mater 55:4041
78. Carlton CE, Ferreira PJ (2007) Acta Mater 55:3749